Water Science & Technology

Water Science & Technology Vol 86 No 1, 211 doi: 10.2166/wst.2022.194

Monitoring PHB production in *Synechocystis* sp. with hyperspectral images

Francisco Rodríguez Lorenzo[a], Miguel Placer Lorenzo[a], Luz Herrero Castilla[b], Juan Antonio Álvarez Rodríguez[b], Sandra Iglesias[a], Santiago Gómez[b], Juan Manuel Fernández Montenegro[a], Estel Rueda[c], Rubén Diez-Montero[d,e], Joan Garcia[d] and Eva Gonzalez-Flo[c,*]

[a] Robotics and Control Unit, AIMEN, Centro de Aplicaciones Láser, Polígono Industrial de Cataboi SUR-PPI-2 (Sector 2) Parcela 3, O Porriño (Pontevedra) 36418, Spain
[b] Environmental Technologies Unit, AIMEN, Centro de Aplicaciones Láser, Polígono Industrial de Cataboi SUR-PPI-2 (Sector 2) Parcela 3, O Porriño (Pontevedra) 36418, Spain
[c] GEMMA-Group of Environmental Engineering and Microbiology, Department of Civil and Environmental Engineering, Escola d'Enginyeria de Barcelona Est (EEBE), Universitat Politècnica de Catalunya-BarcelonaTech, Av. Eduard Maristany 16, Building C5.1, Barcelona E-08019, Spain
[d] GEMMA-Group of Environmental Engineering and Microbiology, Department of Civil and Environmental Engineering, Universitat Politècnica de Catalunya (UPC), c/ Jordi Girona 1-3, Building D1, Barcelona E-08034, Spain
[e] GIA – Group of Environmental Engineering, Department of Water and Environmental Sciences and Technologies, Universidad de Cantabria, Santander, Spain
*Corresponding author. E-mail: eva.gonzalez.flo@upc.edu

EG, 0000-0001-6560-9018

ABSTRACT

Microalgae wastewater treatment systems have the potential for producing added-value products. More specifically, cyanobacteria are able to accumulate polyhydroxybutyrates (PHBs), which can be extracted and used for bioplastics production. Nonetheless, PHB production requires proper culture conditions and continue monitoring, challenging the state-of-the-art technologies. The aim of this study was to investigate the application of hyperspectral technologies to monitor cyanobacteria population growth and PHB production. We have established a ground-breaking measurement method able to discern spectral reflectance changes from light emitted to cyanobacteria in different phases. All in all, enabling to distinguish between cyanobacteria growth phase and PHB accumulation phase. Furthermore, first tests of classification algorithms used for machine learning and image recognition technologies had been applied to automatically recognize the different cyanobacteria species from a complex microbial community containing cyanobacteria and microalgae cultivated in pilot-scale photobioreactors (PBRs). We have defined three main indicators for monitoring PHB production: (i) cyanobacteria specific-strain density, (ii) differentiate between growth and PHB-accumulation and (iii) chlorosis progression. The results presented in this study represent an interesting alternative for traditional measurements in cyanobacteria PHB production and its application in pilot-scale PBRs. Although not directly determining the amount of PHB production, they would give insights on the undergoing processes.

Key words: chlorosis, cyanobacteria, hyperespectral, image processing, PHB, photobioreactor

HIGHLIGHTS

- Hyperspectral technologies allow monitoring cyanobacteria population.
- Spectral measurements differ between growth and PHB-accumulation phases.
- Methodologies definition based on machine learning algorithms allowed on first approach to classify pilot-scale microorganisms and phases.
- Image recognition algorithms permit a visual assessment of chlorosis advance.

GRAPHICAL ABSTRACT

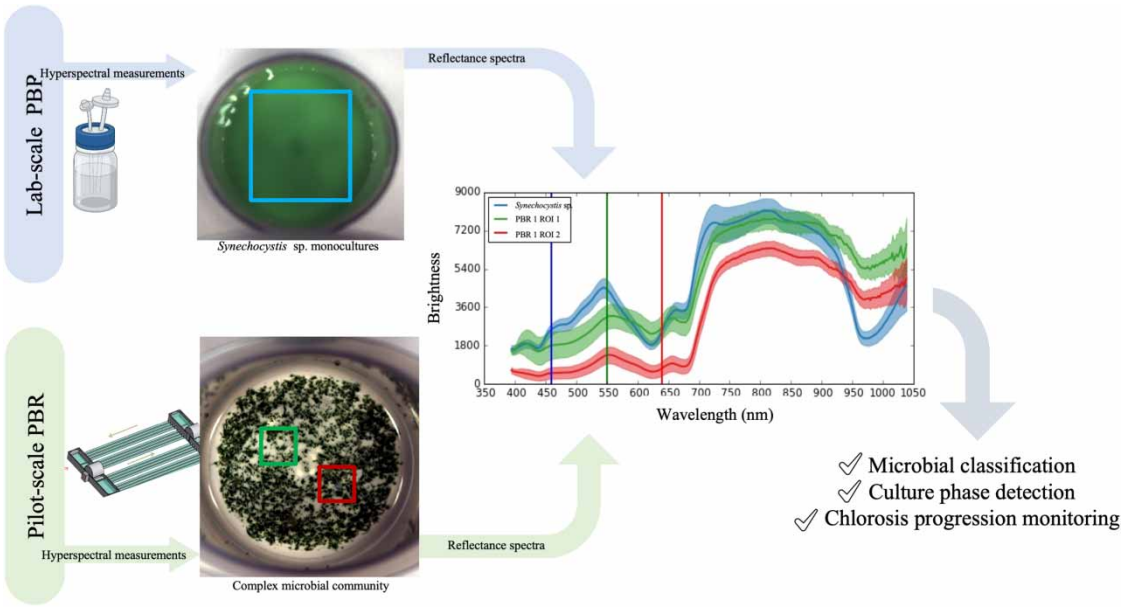

INTRODUCTION

Microalgae-based systems exhibit efficiency for treating different types of wastewaters (García-Galán *et al.* 2020) and producing several added-value products such as nutraceuticals, food additives, biopolymers, pigments, growth promoters, energy (biogas) or biofertilizers among others (Renuka *et al.* 2018; Arashiro *et al.* 2019; Hemalatha *et al.* 2019; Karan *et al.* 2019; Khan *et al.* 2019). A remarkable value-added product that can be obtained from microalgae, specifically from cyanobacteria, is polyhydroxybutyrate (PHB). PHB has become a promising alternative to conventional plastics due to the exhibited similar properties as polypropylene: it is hydrophobic and biocompatible and can be completely biodegraded (Fradinho *et al.* 2013; Drosg *et al.* 2015; Ansari & Fatma 2016; Singh *et al.* 2017; Troschl *et al.* 2017). Coupling of wastewater treatment to PHB production is a bright prospect since it can drastically reduce the PHB production costs. To perform this process, PHB-producing cyanobacteria need first to trigger a series of reactions to eliminate pollutants from wastewater and grow, and secondly, specific cultivation conditions (carbon concentration, nutrient availability, temperature, pH, and redox potential) should be applied to promote polymer accumulation (Montiel-Jarillo *et al.* 2017). Therefore, obtaining economically profitable PHB production requires optimizing cultivation conditions. However, off-line monitoring of key culture parameters (i.e., temperature, pH, and redox potential), is not sufficient for optimizing PHB production.

At-line quantification technologies allowing to determine PHB content in real-time comprise PHA and fluorescence intensity (Choi *et al.* 2015), flow cytometry (Kacmar *et al.* 2005; Karmann *et al.* 2016), photon density wave spectroscopy (Gutschmann *et al.* 2019) or physicochemical analyses (Raman spectrometry, FTIR, SERS) (Hesselmann *et al.* 1999; Almaviva *et al.* 2016; Porras *et al.* 2016; Samek *et al.* 2016; Doppler *et al.* 2021). Although the abovementioned methodologies provide significant benefits for a highly efficient PHB production fail when processes leave the lab and are transferred to pilot plants. Hence, there is the need to obtain a portable and cost-effective monitoring technology satisfying either lab-scale, pilot-scale or industrial-scale requirements. In-situ optical sensors capable of continuously monitoring the PHB producing process represent a promising prospective alternative, allowing to improve the microorganisms' feeding and harvesting cycle for matching the highest PHB concentration.

On the other hand, cyanobacteria present a group of accessory light-harvesting pigment molecules named phycobiliproteins (PBP). PBP pigments are water-soluble and absorb orange and red light near 620 nm, and emit fluorescence at around 650 nm (Sonani *et al.* 2017). Phycocyanin is more difficult to detect in comparison to other pigments due to their lower signal emission and overlapping phenomena with chlorophyll-a, b and c as well as other pigments. A change in pigment content is produced under nitrogen starvation conditions, and simultaneously promoting the accumulation of

PHB granules (Forchhammer & Schwarz 2018). In connection with this, numerous efforts have been done this last decade to detect harmful microalgal blooms (HABs) in aquatic ecosystems caused by the proliferation of cyanobacteria. Most works focused on development of reflectance algorithms and specific spectral index definition for the estimation of chlorophyll-a and phycocyanin concentration or density. Main applications are oriented to remote measurements with images provided by satellite that allows to detect blooms as cyanobacterium *Microscystis* (Beck *et al.* 2017) or estimate cyanobacteria biomass (O'Shea *et al.* 2021). More recently, specific studies combining hyperspectral microscopy and spectroscopy have been developed on characterizing and differentiating several important bloom-forming cyanobacteria to identify species that are prone to produce cyanotoxins (Slonecker *et al.* 2021). Hyperspectral technology improvements opened the door to pigment analysis by fluorescence hyperspectral imaging microscope (Lian *et al.* 2021), pigment localization and distribution in cyanobacterial cells with hyperspectral confocal fluorescence systems (Vermaas *et al.* 2008) or glycogen concentration determination in bioethanol feedstock in *Synechocystis* using a hyperspectral near-infrared imaging system (Ishigaki *et al.* 2016). Although a large number of publications focused on HABs' detection and toxic species identification through advanced technological means (satellites, drones…) and the well-established use of hyperspectral technologies, we report a lack of optical means for monitoring online bioprocess in bioreactors and a reduced number of scientific works using hyperspectral technology for monitoring cyanobacteria in photobioreactors (Havlik *et al.* 2013, 2022). Moreover, there is the need that monitoring systems should be customized to its application, to lower both size and monitoring costs for ensuring a successful integration, and therefore contribute to enhance field and industrial deployment in PBRs.

In step to continuous monitoring cyanobacteria population growth and PHB production, we tested the application of hyperspectral imaging technology. Hyperspectral imaging was chosen due to its versatility and successful applications in the agro-food sector (Govender *et al.* 2007; Li *et al.* 2013). In this study, a cutting-edge methodology allowing *in-situ* and continuous monitoring of cyanobacteria cultures is established. Hyperspectral measurements, machine learning algorithms, and image recognition technologies are combined to automatically recognize cyanobacteria growth and PHB accumulation phases. First hyperspectral measurements had been acquired to lab-scale PBRs. A comprehensive analysis of the spectra obtained from hypercubes during growth and accumulation stages is presented, and variations observed explained relying on bibliography. Moreover, efficient image classification applying unsupervised and supervised techniques based on monoculture spectral signatures allowed to classify pilot-scale microorganisms in either growth or accumulation phase. In essence, the main objectives of this work were: (i) to correlate cyanobacteria density with culture conditions and (ii) cross-check cyanobacteria pigment content change (i.e., due to nitrogen limitation induced chlorosis) with PHB accumulation. The present results are just a small piece of the extensive possibilities of the hyperspectral measurement and its potential application at pilot scale, allowing a more precise live-monitoring estimation of biopolymer accumulation.

METHODS

Strains, media, and growth conditions

The cyanobacteria strain used for lab-scale photobioreactors (PBRs) was *Synechocystis* sp, which was isolated cultured and maintained in BG-11 as described in Rueda *et al.* (2020a). BG-11 consisted of: 1,500 mg·L^{-1} $NaNO_3$, 31.4 mg·L^{-1} K_2HPO_4, 36 mg·L^{-1} $MgSO_4$, 36.7 mg·L^{-1} $CaCl_2{\cdot}2H_2O$, 20 mg·L^{-1} Na_2CO_3, 1 mg·L^{-1} NaMgEDTA, 5.6 mg·L^{-1} citric acid, 6 mg·L^{-1} ferric ammonium citrate and 120 mg·L^{-1} $NaHCO_3$. To prepare a solid medium, BG-11 was supplemented with 1% bacteriological agar. The BG-11 medium and the bacteriological agar were autoclaved separately (at double strength) and mixed when cooled at 50 °C to avoid formation of toxic decomposition products.

A complex microbial community containing cyanobacteria and microalgae were cultivated in pilot-scale PBRs. Cyanobacteria were grown in three full-scale tubular horizontal semi-closed PBRs using and treating agricultural runoff.

Laboratory-scale PBRs

Laboratory-scale PBR experiments were carried out in four 2.5 L PBRs submitted to different inorganic carbon concentrations. The PBRs were closed polymethacrylate cylinders with a diameter of 11 cm and a total volume of 3 L. Each reactor was inoculated with 0.5 L of cyanobacteria culture and 2 L of BG-11 medium. PBRs were continuously agitated with a magnetic stirrer (VELP scientifica, Usmate, Italy) ensuring a complete mixing. Reactors were submitted to 15:9 h light:dark phases and were illuminated by two external 14 W cool-white LED lights providing a medium illuminance of 2.1 klx. Illuminance at different reactor points was measured with a luxmeter (HI 97500, HANNA instruments, Italy). Temperature was regularly measured and maintained at 30 (±2) °C.

Two different phases were applied to each reactor to enhance the PHB accumulation:

(1) Growth phase: N, P and C were added at a concentration that cells could exhaust N and/or P when biomass reached approximately a concentration of 1 g·L^{-1} VSS. The duration of this phase depended on the nutrient uptake rate of each species (from 20 to 30 days). CO_2 injection was used to control pH during this phase. Note that during this phase PBRs were operated in identical conditions (they were in fact replicas).
(2) Accumulation phase: After the growth phase, the mixed liquor of the PBRs was mixed in a tank and divided again in the four reactors to have an identical starting point in accumulation phase. Different culture conditions for inorganic carbon (IC) were established for each PBR as shown in Table 1 to evaluate the effect of inorganic carbon availability in the PHB and glycogen production. The different concentrations of IC were maintained by additions of CO_2 (PBR 1) or HCO_3^- (PBR 2 and PBR 3 as indicated in Table 1). No additions of IC were done in PBR 4. In PBR 1 pH was controlled by means of CO_2 additions. To do so, when pH higher than 9 was detected, an electrovalve was activated an CO_2 was added until pH was around 7–8. In the other PBRs pH was regulated by means of HCl 1M additions. CO_2 was not used in these reactors to avoid excess addition of C and to keep the concentrations of IC indicated in Table 1. The accumulation phase lasted 10 days.

Pilot-scale PBRs: tubular and horizontal semi-closed PBRs

The three PBRs used for a demonstration-scale pilot plant were designed and implemented within the framework of the European project INCOVER 'Innovative Eco-technologies for Resource Recovery from Wastewater' (http://incover-project.eu/ GA 689,242). The plant was located in Agròpolis experimental campus of the Universitat Politècnica de Catalunya-BarcelonaTech (UPC) (41.288 N, and 2.043 E UTM). Detailed information about the PBRs design can be found in García *et al.* (2006).

The pilot-scale PBR in the Agròpolis experimental campus uses wastewater containing a huge diversity of microorganisms including cyanobacteria. The aim is to enhance the growth of specific PHB-producing cyanobacteria. Therefore, different cultivation conditions were applied in the PBRs. Each PBR consisted of two lateral open tanks made of polypropylene connected through 16 low-density polyethylene tubes of 125 mm diameter (Figure 1). They had a useful volume of 11.7 m^3 each (80% within the tubes, 20% in the open tanks). The paddlewheels ensured a proper mixing of the mixed liquor, aiding also to release the excess of dissolved oxygen (DO) that may accumulate within the closed tubes.

Briefly, agricultural runoff was fed to PBR 1, which was devoted to cyanobacteria selection and biomass growth. In PBR 2, inorganic carbon was added in a feast and famine regime to favor PHB-accumulating microorganisms. Finally, inorganic carbon was continuously added in PBR 3 to boost PHB accumulation (Rueda *et al.* 2020b).

Sample collection and analysis

Several samples were collected from the laboratory-scale PBRs and pilot-scale PBRs and analysed with a hyperspectral system as depicted in Figure 2. Hyperspectral measurements were acquired for three consecutive days during the growth phase in lab-scale PBRs, and hyperspectral cubes were taken on the eighth day after the accumulation phase began and lasted for three days. Additionally, hyperspectral cubes had also been acquired during three days on pilot-scale PBRs.

PHB and glycogen analysis

PHB and carbohydrates were measured after each experimental phase. Samples were taken at the beginning of the 15 h light cycle and before C additions. 50 mL of mixed liquor was collected and centrifuged (4,200 rpm, 10 min), frozen at −80 °C overnight in an ultra-freezer (Arctiko, Denmark) and finally freeze-dried for 24 h in a freeze dryer (−110 °C, 0.049 hPa)

Table 1 | Concentrations of IC for each laboratory-scale PBR in the accumulation phase

Parameters	PBR 1	PBR 2	PBR 3	PBR 4
IC, mgC·L^{-1}	>120	20	20	0
CO_2, mgC·L^{-1}	on demand	–	–	–
Daily HCO_3^- additions	–	5.6 mL of HCO_3 2gC L^{-1}	2.8 mL of HCO_3 2gC L^{-1}	0

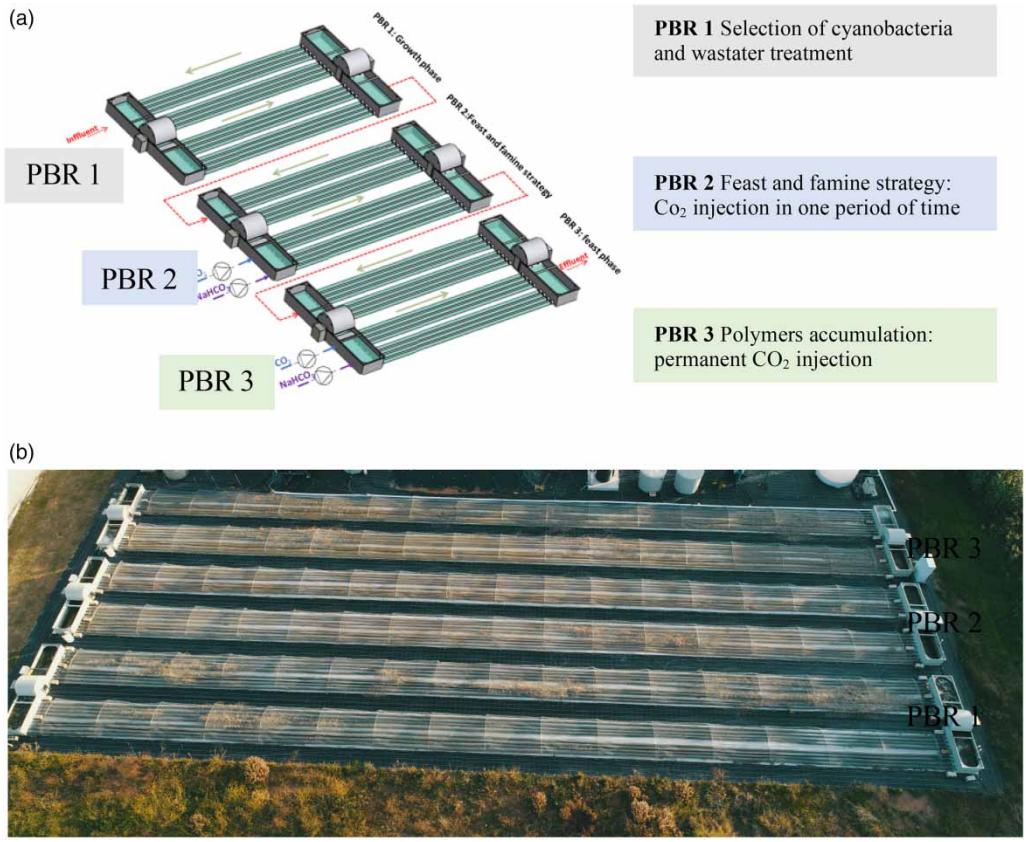

Figure 1 | (a) Scheme of the tubular horizontal semi-closed PBRs' configuration and (b) Agròpolis experimental campus of the Universitat Politècnica de Catalunya-BarcelonaTech (UPC) installations. Red arrows indicate the water flow direction. Green arrows indicate the flux direction inside each PBR. Blue arrows indicate the injection of CO_2.

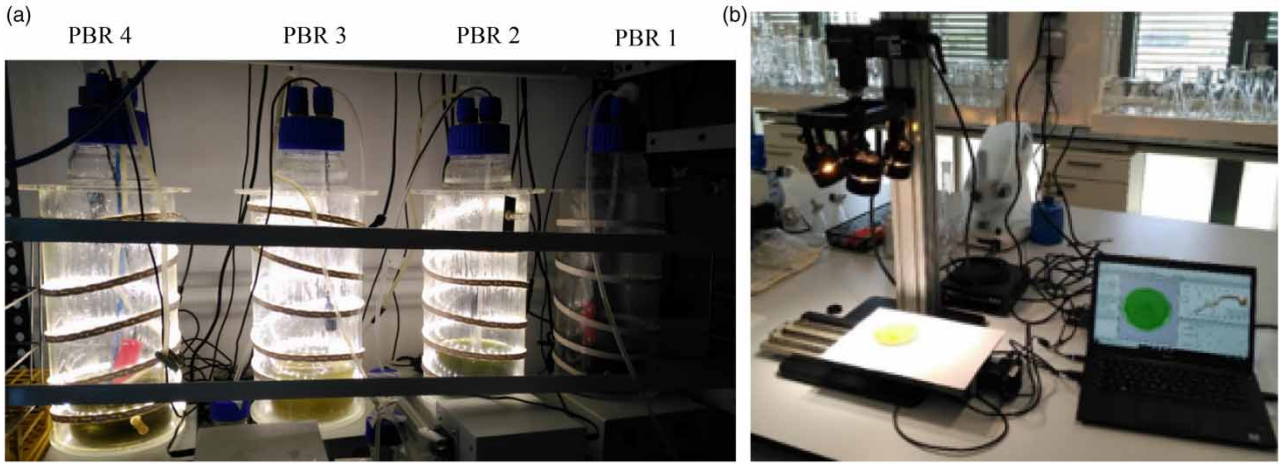

Figure 2 | (a) Laboratory-scale PBRs and (b) hyperspectral equipment deployed for measurements at laboratory scale.

(Scanvac, Denmark). PHB extraction and analysis were adapted from the methodology described by Lanham *et al.* (2013). Briefly, 1 mL of MeOH acidified with H_2SO_4 (20% v/v) and 1 mL of $CHCl_3$ containing benzoic acid as internal standard were added to 2–3 mg of lyophilized biomass. Tubes were then incubated in a dry-heat thermo-block (Selecta, Spain) during 5 h at 100 °C. After that, they were rapidly cooled on ice for 30 min and 0.5 mL of deionized water were added to

each tube. Afterwards, they were vortexed for 1 min to separate the different solvents by density. $CHCl_3$ was removed with a Pasteur pipette and placed into a vial with molecular sieves to remove the water that could remain in the sample. PHB was determined by means of gas chromatography (GC) (7820A, Agilent Technologies, USA). It was quantified measuring the PHB monomer hydroxybutyrate (HB) and hydroxyvalerate (HV), using the co-polymer of PHB-PHV as a standard. A calibration curve with six points was prepared and processed in the same way as the samples.

Carbohydrate extraction was done following the methodology described by Lanham *et al.* (2012) and concentration was measured using the phenol–sulfuric acid method described by Dubois *et al.* (1956). Briefly, 2 mL of HCl (1 N) were added to 1–2 mg of freeze-dried biomass, and then the tubes were incubated in a dry-heat thermo-block (Selecta, Spain) at 100 °C for 2 h. Samples were left to cool down to room temperature (approximately 15 min) and then 0.5 mL of 5 %w/v phenol solution and 2.5 mL of H_2SO_4 were added to the tubes. They were vortexed, left to rest for 10 min and finally placed in a bath at 35 °C for 15 min. Eventually, the absorbance at 492 nm was measured by a spectrophotometer (Spectronic Genesys 8, Spectronic instrument, UK). Cyanobacteria synthetize carbohydrates as glycogen (Markou *et al.* 2012). Therefore, it was considered that carbohydrates measured with this method were mainly in form of glycogen. However, the analytical methodology used not only measured glycogen but also all the polysaccharides formed by glucose monomers, such as polysaccharides of the cell wall and the excreted exopolysaccharides.

Hyperspectral technology

Measurements were applied to laboratory-scale and pilot-scale PBR samples with the Pika L camera system from Resonon based on push broom technology. A detailed scheme of the technology is shown in the supplementary material Figure A1. It consists of a small and compact hyperspectral sensor adapted to field measurements. Its compact design and rugged structure allow a good integration in several platforms, such as laboratory workbench, outdoor rotary scanning system or drone systems. The sensor covers a spectral range from 400 to 1,000 nm, with 281 spectral channels and a resolution of 2.1 nm. Sensor has a quantum efficiency higher than 55% (55% @ 700 nm and reaching more than 70% between 500 and 600 nm). Global system quantum efficiency (Q.E.) is higher than 55% in the range from 500 to 600 nm. A 20 mm focal lens objective allowed working directly on samples collected directly from the PBRs. For analysis and acquisition, Spectronon software from Resonon was used, as it has a complete library with image processing tools (as support vector machine, hyperspectral vegetation indices, region of interest cropping tools, among others) and allows integration of Python customized plugins.

Calibration and image parameter adjustment

After adjusting focus, a dark current and absolute reflectance reference are acquired. The collection of multiple dark frames was used to subtract the dark current noise from measurements. For absolute reflectance a reference sheet of white Teflon® was used. Aspect ratio and acquisition parameters were then applied as shown in Table 2.

RESULTS AND DISCUSSION

Hypercube acquisition and interpretation in laboratory-scale PBR cyanobacteria monocultures

To develop a novel methodology for differentiating between cyanobacteria and other microorganisms, and to estimate cyanobacteria population density for *in vivo* cultures, phycocyanin reflectance variations were tracked in both growth and

Table 2 | Aspect ratio, and image acquisition parameters for measurements set

Parameters	Value
Scanning speed, cm/s	0.25
Homing speed, cm/s	1
Jog speed, cm/s	2
Framerate, Hz	20
Integration time, ms	6
Gain	12

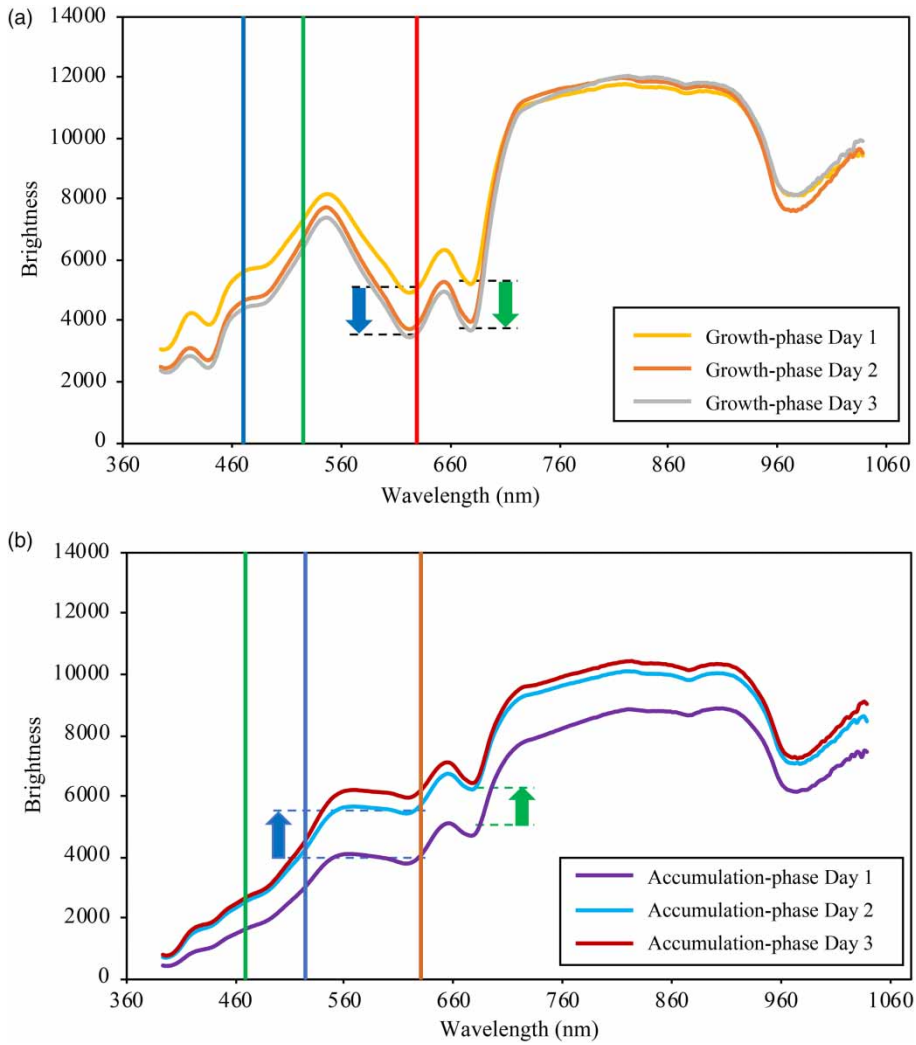

Figure 3 | Mean reflectance spectra for lab-scale PBR 1 containing *Synechocystis* sp. monocultures for three consecutive days. Vertical lines represent the reflectance peak for blue, green and red color, respectively. Standard deviation is not plotted here for improving visualization). (a) growth-phase reflectance spectra for three consecutive days (b) and accumulation phase reflectance spectra for three consecutive days starting at the eighth day after accumulation started.

accumulation phases for laboratory-scale PBRs. Figure 3(a) shows the spectra obtained from the hypercube captured for three consecutive days during the growth phase for *Synechocystis* sp. Each spectrum is plotted considering a region of interest (ROI) in the image of 400×350 pixels. We can localize the spectral response of phycocyanin and chlorophyll-a pigments at 620 and 670 nm, respectively. Notice that higher absorption of phycocyanin and chlorophyll-a is obtained as growth phase progresses.

Extracting direct reflectance values from 620 nm allows plotting the phycocyanin reflectance variations level during consecutive days of the growth phase. A clear trend correlating the phycocyanin reflectance and cyanobacteria growth is observed in Supplementary material Figure A2. Although only a few measurement points were carried out to establish the correlation, it suggests the possibility of monitoring the growth phase by phycocyanin reflectance. In this first analysis, the effect of chlorophyll-a pigment on reflectance values at 620 nm had not been considered. Further analysis would comprise a prior calibration stage to get a quantitative estimation of phycocyanin concentration. Calibration would require a standard solution with pure extracted phycocyanin with and without chlorophyll-a combined with data from a cyanobacteria growing population. Hence, it would allow establishing a stronger correlation between phycocyanin reflectance values and cyanobacteria populations.

Similar to the growth phase, hyperspectral images have been acquired during the accumulation phase for three days following the same methodology (same 400 × 350 pixels ROI for data cube analysis). In Figure 3(b) it can be observed a clear difference from the growth phase spectra. The reflectance peak at 540 nm, characteristic of blue-green light, is less intense and sharp than for the spectra obtained during the growth phase. Phycocyanin and chlorophyll-a absorption decrease and general reflectance level in visible spectral band increases. This tendency was observed for all PBRs (Figure A3). This effect can be partially explained by nitrogen depletion and subsequent chlorosis (Troschl *et al.* 2017). In our experiments 95% of the phycocyanin was degraded within 24 hours and chlorophyll-a was degraded after 10 days. As hyperspectral measurements started on the 36th day of the experiment (i.e., eight days after the accumulation phase began) an important percentage of phycocyanin and chlorophyll-a pigments had been degraded.

Phycocyanin reflectance values were extracted from three consecutive days of the accumulation phase and plotted in Figure A4. Phycocyanin variation for PBR 1 and PBR 2 show a temporal correlation, a logarithmic progression is the best tendency fitting the data. Phycocyanin and chlorophyll-a absorption reduction is also observed in PBR 3 and 4, and seem to have a same tendency, although, patterns are not the same. Further studies should be done to determine an empirical law that could fit, with an acceptable regression coefficient.

Furthermore, nitrogen chlorosis evolution can also be monitored by plotting phycocyanin to chlorophyll-a ratio (PC/Ch-a) (Damrow *et al.* 2016). Phycocyanin and cholorophyll-a absorption rates were extracted from the reflectance spectrum at 620 and 680 nm respectively. PHB and Glycogen concentrations were obtained from the accumulation phase and progression of nitrogen chlorosis was plotted in Figure A5. The lower the PC/Ch-a ratio, the more advanced the chlorosis is. Considering the tendency curves from the presented points, it seems that the increase and decrease of PHB and glycogen production rates are interrelated. It has been previously demonstrated that a disruption in PHB synthesis results in an increased glycogen production. However, the reverse effect, i.e., an overproduction of glycogen, does not lead to higher amounts of PHB (Koch *et al.* 2019). Explanation of mechanisms of the glycogen and PHB production accumulation exchanges is to the date actively investigated and part of the metabolic pathways is still unclear (Koch *et al.* 2019).

Hypercube acquisition and interpretation in pilot-scale PBRs (complex microalgae-bacteria communities)

The hyperspectral analysis has to consider the diversity and complexity of the microalgae-bacteria communities of the pilot PBR samples, as different spectra can be extracted from the hypercubes. Previous measurements obtained in *Synechocystis* sp. lab-scale monocultures were considered as reference values, and its reflectance spectrum was compared with the spectra obtained from pilot-scale PBRs (Figure 4). In more detail, *Synechocystis* sp. measurements in the growth phase were acquired in hypercube at the same time as samples from pilot-scale PBR 1. Pilot-scale samples were not a homogeneous culture (in contrast to *Synechocytis* sp. cultures) and spontaneous flocculation created aggregates which enclosed different cyanobacteria species, eukaryotic microalgae and bacteria. In Figure 4 the spectra from pilot-scale PBR 1 obtained from different ROIs are shown. The spectra from pilot-scale PBRs show differences compared with the reference *Synechocystis* sp. lab-scale spectrum. The main differences arise in the intensity and sharpness of the reflectance peak located at 540–550 nm band and reflectance values at 620, 650 and 680 nm. The stretching effect depicted between 540 and 550 nm is mainly due to differences in cyanobacteria concentration compared with the laboratory-scale PBRs, but also due to the variability in specific cyanobacteria specific pigments concentration (i.e., phycocyanin, phycoerythrin and allophycocyanin) of other cyanobacteria species present in the sample of the pilot PBRs (Wojtasiewicz & Stoń-Egiert 2016). This fact leads to spectral mixing providing the reflectance shape and level observed in this spectral band. Moreover, reflectance spectra obtained at any point in the red green blue (RGB) image are located between two spectra limits (green and red).

The same methodology has been applied to two samples extracted from PBR 2 and PBR 3 (see Figure A6 in supplementary information). Main characteristics from different chlorotic status can be deduced from the spectra. The evolution of different quoted reflectance peaks and absorption of pigments from photosynthetic systems are shown in the Figure 5. A shift from green to brown color, which is a visible aspect of chlorosis, can be seen on the spectra. The reflectance spectrum with a peak at 540 nm (sample from PBR 1) shifts to 560 nm, and the reflectance value increases in the red band at 630 nm (sample from PBR 3). Reflectance absorption which was observed initially at 620 nm and which is characteristic from phycocyanin absorption disappeared in PBR 3 sample. Moreover, absorption due to chlorophyll-a was also reduced. Notice that an important absorption appears in the near infrared region at 800 and 870 nm in the samples extracted from PBR 3 with unknown origin.

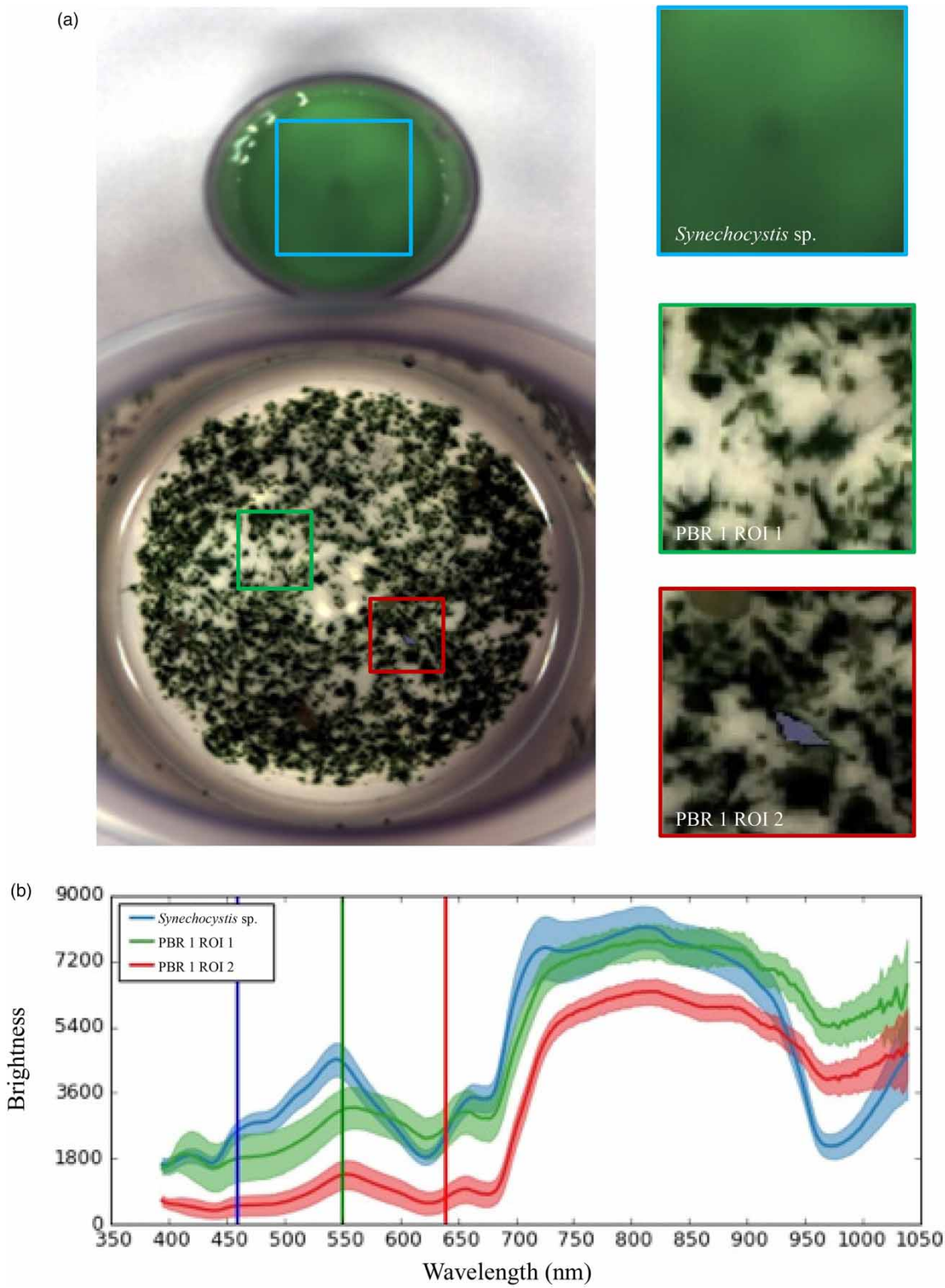

Figure 4 | Comparison between reflectance spectrum of *Synechocystis* sp. from lab-scale PBR and spectra obtained in two different areas from pilot-scale PBR 1. (a) Image of a sample from *Synechocystis* sp. monocultures (top petri dish) and image of a sample from pilot-scale PBR 1 (bottom petri dish). Different selected ROIs corresponding to *Synechocystis* sp. monoculture (blue square) and pilot-scale PBR 1 (green and red squares). (b) Mean reflectance spectra for lab-scale PBR containing *Synechocystis* sp. monocultures obtained during the growth phase and the two selected ROIs for pilot-scale PBR 1 sample.

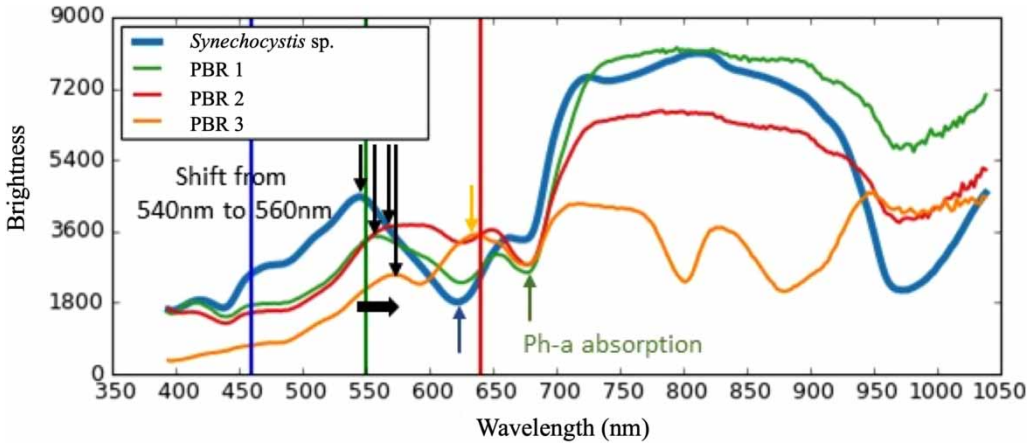

Figure 5 | Evolution of reflectance peak in the green band and phycocyanin and chlorophyll-a absorption in samples from pilot-scale PBRs. Vertical lines represent the reflectance peak for blue, green and red color, respectively.

Information from pilot-scale PBRs and process indicator definition with machine learning algorithms

As previously observed (data not shown) that it is possible to identify by our spectra methods different states for cyanobacteria; i.e., growth and accumulation stage. Indeed, spectra shape and photosynthetic pigments variations (as phycobiliproteins or chlorophyll-a) can be monitored at specific wavelengths. The main challenge relies on the selection and separation of useful information in samples without any kind of chemical pre-treatment. In this section is present different image processing approaches for classification and extraction of information from the hyperspectral data, Figure A7 from supplementary materials outlines the established workflow. In essence, two different machine learning algorithms were used. An unsupervised clustering algorithm, k-means, was used to identify all the pixels with similar spectral characteristics, for instance, detection of *Synechosystis* sp. pixels. On the other hand, a supervised classification algorithm, Spectral Angle Mapper (SAM), allowed classification of the growth and accumulation phases based on spectral similarities using the spectra obtained from *Synechosystis* sp monoculture as a reference.

The k-means clustering algorithm was applied to make a first classification of the hyperspectral images obtained from samples in pilot-scale PBRs. The k-means unsupervised classification algorithm calculates initial class means evenly distributed in the data space, then iteratively clusters the pixels into the nearest class using a minimum-distance technique. In each iteration recalculates class means and reclassifies pixels to the new means. Figure 6 shows classification obtained by the k-means algorithm with six layers. For each image the top petri dish corresponds to the laboratory-scale PBR sample in growth phase and the bottom petri dish to pilot-scale PBRs 1, 2 and 3, respectively. In the colormaps the pixels with spectral similarities are plotted with the same color. The algorithm identifies and classifies pixels for pilot-scale PBRs. Pixels that have the same spectral properties as the reference sample (i.e., *Synechosystis* sp. from lab-scale PBR in growth phase). Notice that the algorithm detects pixels with more spectral similarity in PBR 1 (bluish and purplish regions) than PBR 2, and no similarity is found in PBR 3. This is coherent with the PBRs' performance, as it is expected that there will be more cyanobacteria in the growth stage, corresponding to pilot-scale PBR 1. Intuitively, we can forecast that the spectra obtained in PBR 1 will be more similar to a reference sample than the spectra extracted from PBR 3 (Figure A6). Furthermore, PBR 3 corresponds to the accumulation culture conditions, hence the spectra shape should be different when compared to reference one. The k-means algorithm can be used as the first automatic classifier, establishing an adequate number of classes (i.e., layers) and iterations. An adequate adjustment of classification criteria and similarity metrics is also necessary, as the algorithm can be sensitive to glare effects. Notice that to optimize image processing it is necessary to adjust the density of aggregates in the sample. A sample with high aggregate density gives difficult image clustering; however, this can be solved by spreading aggregates in a single layer at the bottom of the petri dish.

A supervised classification algorithm was tested as a second approach. SAM uses an n-D angle to match pixels to reference spectra or trained pixels. The algorithm determines the spectral similarity between two spectra by calculating the angle between the spectra and treating them as vectors in a space with dimensionality equal to the number of bands. In the first classification, we have used as reference spectra obtained from the hypercube captured for three days during the growth stage (Figure 1(a)). Three samples from the *Synechocystis* sp. monoculture in a laboratory-scale PBR were used for training

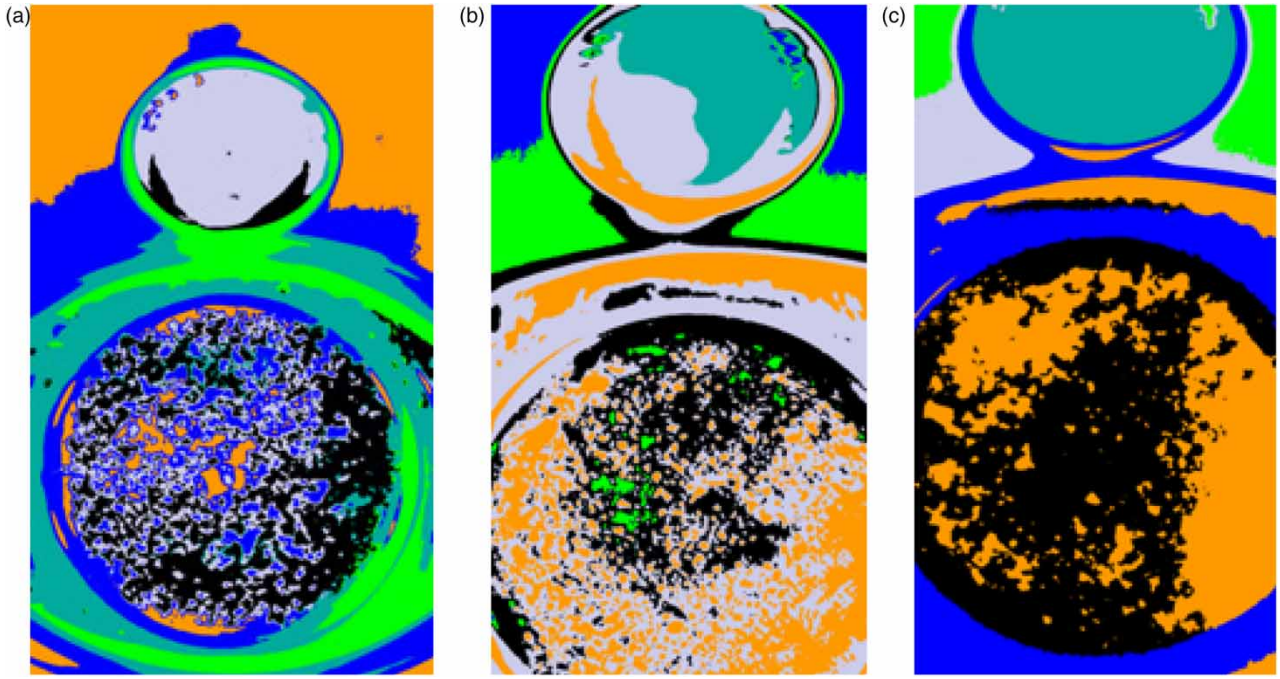

Figure 6 | Classification maps obtained from k-means clustering algorithm applied to hyperspectral images obtained from samples in pilot-scale (a) PBR 1, (b) PBR 2 and (c) PBR 3. *Synechosystis* sp. sample from laboratory-scale PBR (top petri dish) for comparison and pilot-scale PBR sample (bottom petri dish).

the algorithm and three samples from the pilot-scale PBR 1 for testing, as samples collected from pilot-scale PBR 1 are supposed to be in the growth phase due to enough nutrient rate. As can be seen in Figure 7, the SAM algorithm allows detecting pixels that have spectra close to the reference spectra. Additional measurements at the laboratory scale in the growth phase should allow better evaluation of the resolution time and sensitivity of the system, i.e., the smallest reflectance variation that is detectable in the smallest time variation. Similarly, the SAM algorithm was applied to samples collected from pilot-scale PBR 2 using as reference spectra obtained from the hypercube captured for three days during the accumulation stage (Figure 1(b)). The SAM algorithm finds some similarities in the pixel spectra; however, a lower quantity of detected area suggests that cyanobacteria in the pilot-scale sample are in a different growth phase. In pilot-scale PBR 2, a feast and famine strategy was imposed; hence, it is possible that a part of the culture was still in a growth phase and the other had already entered chlorosis.

Chlorosis progression monitoring

As analysed for the laboratory-scale PBRs, chlorosis progression indicator is defined as the ratio between phycocyanin absorption at 620 nm and chlorophyll-a absorption at 680 nm. For the pilot-scale PBRs this ratio was computed in a grayscale image (Figure 8), providing a visual assessment of chlorosis advance. White pixels indicate the area where there is a higher phycocyanin absorption and thus concentration. The three pilot-scale PBRs show a clear change in the ratio, as starvation starts in PBR 2, the concentration of the photosynthetic pigments as phycocyanin decrease dramatically, corresponding to a decrease of white pixels density in the inverted grayscale images in Figure 8(b) and 8(c). Furthermore, the depicted behaviour corresponds with the feast and famine culture conditions applied to the PBR 2. Phycocyanin absorption decreases and the density of white pixels is lower than in PBR 1 (Figure 8(a)). In the PBR 3, shown in Figure 8(c), in PHB accumulation conditions, chlorosis is found in an advanced stage. Doubtless, all phycocyanin pigments would be practically degraded and photosynthetic activity minimized, resulting in the dark pixels from Figure 8(c).

Moreover, the estimated percentage of chlorosis advance for a region of interest in each image has been computed considering the number of dark pixels compared to the total number of pixels associated with biomass (i.e., white and dark pixels associated with aggregates). Images have been binarized to separate background pixels from useful pixels. Extracted information has been reported in Table 3. We have estimated per each ROI the percentage of dark pixels corresponding to an area with a low or minimal level of phycocyanin and thus in an advanced chlorosis state. The total pixels used for computing

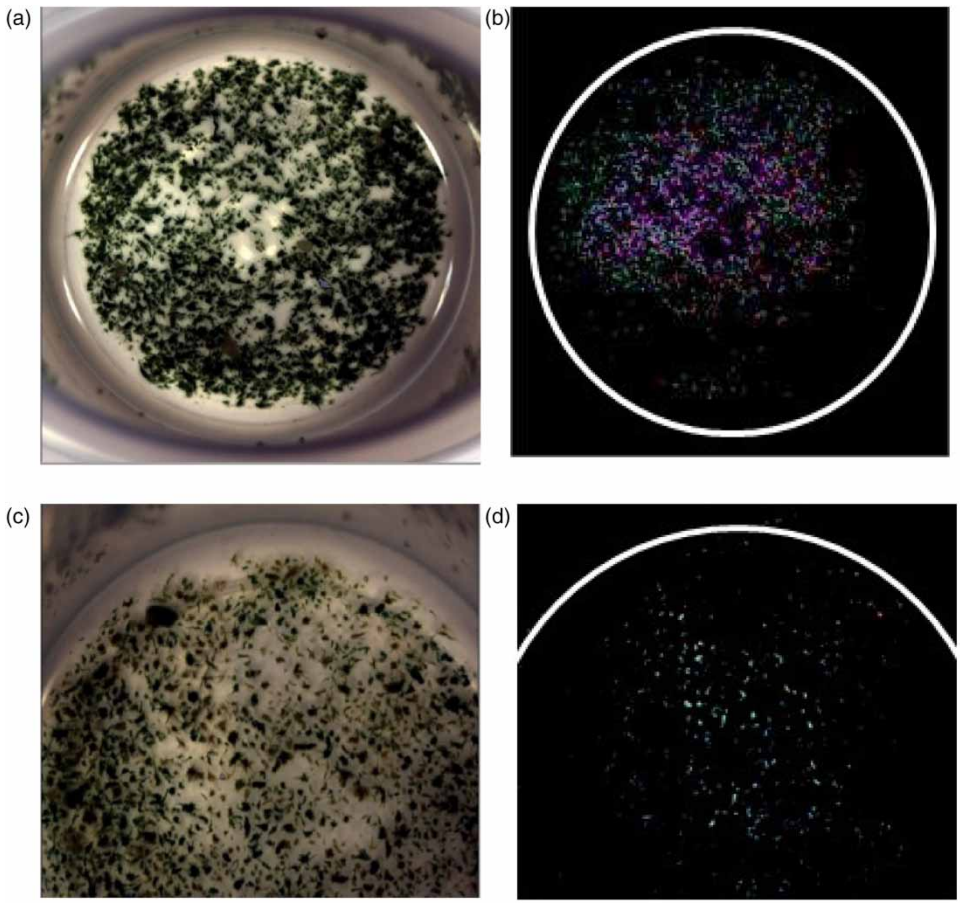

Figure 7 | SAM algorithm colormap applied to pilot-scale PBR 1 and PBR 2. (a) Pilot-scale PBR 1 sample. (b) Colormap from SAM algorithm for Pilot-scape PBR 1 sample. (c) Pilot-scape PBR 2 sample. (d) Colormap from SAM algorithm for Pilot-scape PBR 2 sample. Spectra obtained during the growth phase for *Synechosystis* sp. at lab-scale PBR was taken as reference. Green (first day), red (second day), blue (third day) areas correspond to similarities with reference spectra. White contouring circles have been added to facilitate visual localization of petri dish limits.

are the pixels corresponding to aggregated areas, where cells, cyanobacteria or other species are concentrated. As we can see, the more advanced the chlorosis is, the higher the ratio of DP/TPa is. Although these indicators would not directly determine the amount of PHB production, they would give insights on the processes of growing and accumulation.

CONCLUSIONS

Microalgae have been revealed as a powerful technology coupling wastewater treatment together with the production of added-value goods. Nonetheless, there are still some challenges regarding the production process since cultivation conditions for the accumulation of biopolymers are very specific and culture-dependent. The necessity for continuous monitoring of the culture means it is difficult for the process to be economically profitable and scalable outside laboratory conditions. The methodology presented in this study combines the acquisition of spectral light emitted from cyanobacteria during growth and accumulation phases together with classification algorithms. The present methodology allows defining three main indicators for monitoring PHB production: the first one allows estimation of specific cyanobacteria in complex bacteria communities, the second one allows differencing growth from accumulation stage, and the last permits an easy way for chlorosis progression monitoring. Although the indicators would not directly determine the amount of PHB production, they would give insights on the processes of growing and accumulation. The present results are just a small piece of the potentially far-reaching possibilities of hyperspectral measurement and the potential application uses at pilot scale, allowing more precise live-monitoring estimation of biopolymer accumulation. Indeed, the present study has been conducted on a reduced number of samples, three samples from *Synechocystis* sp. monoculture during growth phase and 12 during the accumulation

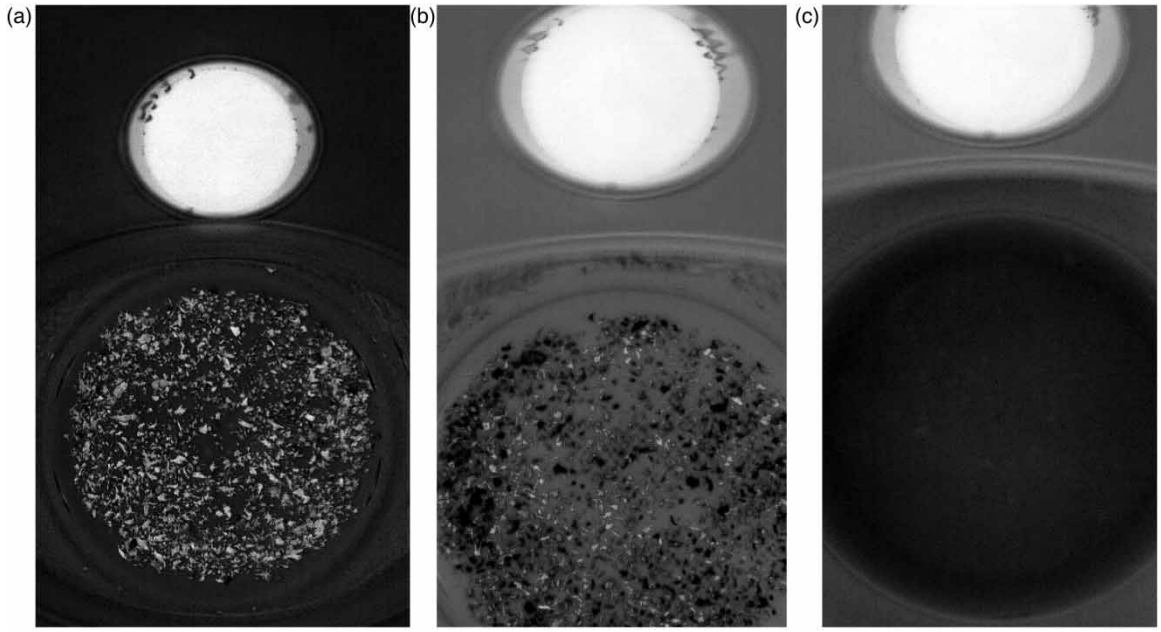

Figure 8 | Grey scale images obtained from reflectance ratio (PC/Ch-a) of pilot-scale PBR samples. (a) PBR 1, (b) PBR 2 and (c) PBR 3. White pixels indicate a higher level of phycocyanin absorption compared to chlorophyll. Spectra obtained during the growth phase for *Synechosystis* sp. at lab-scale PBR was taken as a reference Image is shown in grey inverted scale.

Table 3 | Estimation of PC/Ch-a ratio from pilot-scale PBR samples

Parameter	PBR 1	PBR 2	PBR 3
White pixels number (WP)	81,114	11,714	675
Dark pixels number (DP)	160,283	71,574	87,299
Total pixels number (TP)	241,397	471,104	578,088
Pixels number of aggregates (TPa)	81,114	83,288	87,974
DP/TPa	0	0.86	0.96

phase in laboratory-scale PBRs, and three samples from pilot-scale PBRs. An extended number of samples are needed to validate first analysis and tendencies and to further establish a robust statistical assessment.

Departing from monoculture spectra of known species in laboratory conditions allows differentiating the different cyanobacteria species in pilot-scale PBRs. To reinforce our proposed methodology, further measurements for establishing a spectral comparison with other species are necessary. Efficient classification and segmentation based on spectral signatures can then be performed. Estimation of density can be achieved by counting pixels in the image ROI identified where cyanobacteria or specific species are detected. Specifically, for *Synechocystis* sp, this is linked to spectral emission at 540 nm, and the presence of phycocyanin absorption at 620 nm. With a microscopic identification and counting process (CFU process) for a defined area, it is possible to extrapolate and estimate global concentration in the sample. This characterization step should be used for a labeling process providing input data for the development of a training strategy for a machine learning-based software. This data set should constitute a ground truth for classifier development and validation.

The second indicator allows differentiating between growth and accumulation phases. Laboratory-scale PBRs with *Synechocystis* sp. spectra obtained during growth and accumulation phases depict clear different shapes making it possible to identify each process stage. With complimentary measurements, it could be also possible to estimate the remaining time between stages. Together with the last indicator based on the PC/Ch-a ratio, it should allow to estimate PHB accumulation progression. To our knowledge, this comparison approach between a specific monoculture from a laboratory PBR and

complex microalgae-bacteria comminutes sampled in field PBRs has not been enough addressed with a hyperspectral system deployed in local configuration. The main benefit of the presented methodology is a first step to being able to quantify specific cyanobacteria species in complex bacteria communities by retrieving a density estimation and thus contribute to field PBR optimization in real time. At least, chlorosis indicators associated to a gray scale images representation are shown for helping users to estimate accumulation progression intuitively.

Efforts should be made on developing specific sensors that could be deployed in laboratory-, pilot- or industrial-scale PBRs at a low and effective cost. From a hardware point of view, expansive complex hyperspectral systems can be substituted by multispectral sensors fitted with a specific filtering system (e.g., filter wheels or fixed optomechanical filter mounting) centered on a spectral band of interest. On the other hand, from a software perspective, algorithms obtained from classifier training could then be implemented on a Single Board Computer or even smart cameras, hence IoT technologies and visions systems are reaching a high processing speed and robustness maturity levels for a reduced cost allowing an affordable integration in PBRs. Furthermore, other options for assessment are normalized spectral indices for quantifying carbon and nitrogen concentration. These spectral indices (SI) have been developed mainly for image processing obtained from remote sensing systems and applied to precision agriculture for example corn crop monitoring (Chen *et al.* 2010). In our case, an estimation of nitrogen quantity could allow determining the beginning of the accumulation stage. Monitoring carbon would provide information to the operator that could ensure that carbon feeding is constant all along the process. Tests are also currently being done to evaluate if SI is applicable in our case. Recently, we can point out that new spectral indices have been developed in the SWIR spectral region (Herrmann *et al.* 2010; Camino *et al.* 2018), with improved nitrogen and carbon estimation; but as actual acquired hyperspectral images are in the VNIR range, these indices could not be applied in our case. Moreover, with the presented methodology, chlorosis progression has been also monitored both for laboratory-scale and pilot-scale PBRs providing a visual assessment of chlorosis advance. In summary, *in-situ* hyperspectral data could represent an interesting alternative for traditional analytical measurement allowing for continuous culture monitoring based on optical sensors technology.

ACKNOWLEDGEMENTS

This research was funded by the European Union H2020 Research and Innovation program [INCOVER, GA 689242] and [PROMICON, GA 101000733]. R. Díez-Montero would like to thank the Spanish Ministry of Economy and Competitiveness for his research grant (FJCI-2016-30997). E. Rueda would like to thank the Spanish Ministry of Education, Culture and Sport for her grant (FPU18/04941). E. Gonzalez-Flo would like to thank the European Union-NextGenerationEU, Ministry of Universities and Recovery, Transformation and Resilience Plan for her research grant (2021UPF-MS-12). The dissemination of results herein reflects only the author's view and the Commission is not responsible for any use that may be made of the information it contains. Special thanks to Ramón Villanova, Photon Lines Óptica, S.L., for providing the Pika L camera and linear stage equipment.

DATA AVAILABILITY STATEMENT

All relevant data are included in the paper or its Supplementary Information.

CONFLICTS OF INTEREST STATEMENT

The authors declare there is no conflict.

REFERENCES

Almaviva, S., Palucci, A. & Botti, S. 2016 Validation of a miniaturized spectrometer for trace detection of explosives by surface-enhanced Raman spectroscopy. *Challenges* **7**, 14.

Ansari, S. & Fatma, T. 2016 Cyanobacterial polyhydroxybutyrate (PHB): screening, optimization and characterization. *PLoS One* **11**, 1–20.

Arashiro, L. T., Ferrer, I., Rousseau, D. P. L., Van Hulle, S. W. H. & Garfí, M. 2019 The effect of primary treatment of wastewater in high rate algal pond systems: biomass and bioenergy recovery. *Bioresour. Technol.* **280**, 27–36.

Beck, R., Xu, M., Zhan, S., Liu, H. & Johansen, R. A. 2017 Comparison of satellite reflectance algorithms for estimating phycocyanin values and cyanobacterial total biovolume in a temperate reservoir using coincident hyperspectral aircraft imagery and dense coincident surface observations. *Remote Sens.* **9** (6), 538. https://doi.org/10.3390/rs9060538.

Camino, C., González-Dugo, V., Hernández, P., Sillero, J. C. & Zarco-Tejada, P. J. 2018 Improved nitrogen retrievals with airborne-derived fluorescence and plant traits quantified from VNIR-SWIR hyperspectral imagery in the context of precision agriculture. *Int. J. Appl. Earth Obs. Geoinf.* **70**, 105–117. https://doi.org/10.1016/j.jag.2018.04.013.

Chen, P., Haboudane, D., Tremblay, N., Wang, J., Vigneault, P. & Li, B. 2010 New spectral indicator assessing the efficiency of crop nitrogen treatment in corn and wheat. *Remote Sens. Environ.* **114** (9), 1987–1997. https://doi.org/10.1016/j.rse.2010.04.006.

Choi, J. E., Na, H. Y., Yang, T. H., Rhee, S. K. & Song, J. K. 2015 A lipophilic fluorescent lipidgreen1- based quantification method for high-throughput screening analysis of intracellular poly-3-hydroxybutyrate. *AMB Express* **5**, 131.

Damrow, R., Maldener, I. & Zilliges, Y. 2016 The multiple functions of common microbial carbon polymers, glycogen and PHB, during stress responses in the non-diazotrophic cyanobacterium Synechocystis sp. PCC 6803. *Front. Microbiol.* **7**, 966. doi:10.3389/fmicb.2016.00966. eCollection 2016.

Doppler, P., Gasser, C., Kriechbaum, R., Ferizi, A. & Spadiut, O. 2021 In situ quantification of polyhydroxybutyrate in photobioreactor cultivations of Synechocystis sp. using an ultrasound-enhanced ATR-FTIR spectroscopy probe. *Bioengineering* **8**, 129. https://doi.org/10.3390/bioengineering8090129.

Drosg, B., Fritz, I., Gattermayr, F. & Silvestrini, L. 2015 Photo-autotrophic production of poly(hydroxyalkanoates) in Cyanobacteria. *Chem. Biochem. Eng. Q.* **29**, 145–156.

Dubois, M., Gilles, K. A. & Hamilton, J. K. 1956 Colorimetric method for determination of sugars and related substances. *Anal. Chem.* **28**, 350–356.

Forchhammer, K. & Schwarz, R. 2018 Nitrogen chlorosis in unicellular cyanobacteria – a developmental program for surviving nitrogen deprivation. *Environ. Microbiol.* **21** (4), 1173–1184.

Fradinho, J. C., Domingos, J. M., Carvalho, G., Oehmen, A. & Reis, M. A. 2013 Polyhydroxyalkanoates production by a mixed photosynthetic consortium of bacteria and algae. *Bioresour. Technol.* **132**, 146–153. doi:10.1016/j.biortech.2013.01.050.

García, J., Green, B. F., Lundquist, T., Mujeriego, R., Hernández-Mariné, M. & Oswald, W. J. 2006 Long term diurnal variations in contaminant removal in high rate ponds treating urban wastewater. *Bioresour. Technol.* **97**, 1709–1715. https://doi.org/10.1016/j.biortech.2005.07.019.

García-Galán, M. J., Arashiro, L., Santos, L. H. M. L. M., Insa, S. G., Rodríguez-Mozaz, S., Barceló, D., Ferrer, I. & Garfí, M. 2020 Fate of priority pharmaceuticals and their main metabolites and transformation products in microalgae-based wastewater treatment systems. *J. Hazard. Mater.* **390**, 121771.

Govender, M., Chetty, K. & Bulcock, H. 2007 A review of hyperspectral remote sensing and its application in vegetation and water resource studies. *Water SA* **33** (2). doi:10.4314/wsa.v33i2.49049.

Gutschmann, B., Schiewe, T., Weiske, M. T., Neubauer, P., Hass, R. & Riedel, S. L. 2019 In-line monitoring of polyhydroxyalkanoate (PHA) production during high-cell-density plant oil cultivations using photon density wave spectroscopy. *Bioengineering* **6**, 85. doi:10.3390/bioengineering6030085.

Havlik, I., Lindner, P., Scheper, T. & Reardon, K. F. 2013 On-line monitoring of large cultivations of microalgae and cyanobacteria. *Trends Biotechnol.* **31** (7), 406–414.

Havlik, I., Beutel, S., Scheper, T. & Reardon, K. 2022 On-line monitoring of biological parameters in microalgal bioprocesses using optical methods. *Energies* **15** (3), 875. https://doi.org/10.3390/en15030875.

Hemalatha, M., Sravan, J. S., Min, B. & Venkata Mohan, S. 2019 Microalgae-biorefinery with cascading resource recovery design associated to dairy wastewater treatment. *Bioresour. Technol.* **284**, 424–429.

Herrmann, I., Karnieli, A., Bonfil, D. J., Cohen, Y. & Alchanatis, V. 2010 SWIR-based spectral indices for assessing nitrogen content in potato fields. *Int. J. Remote Sens.* **31** (19), 5127–5143. https://doi.org/10.1080/01431160903283892.

Hesselmann, R. P. X., Fleischmann, T., Hany, R. & Zehnder, A. J. B. 1999 Determination of polyhydroxyalkanoates in activated sludge by ion chromatographic and enzymatic methods. *J. Microbiol. Methods* **35**, 111–119.

Ishigaki, M., Nakanishi, A., Hasunuma, T., Kondo, A., Morishima, T., Okuno, T. & Ozaki, Y. 2016 High-speed scanning for the quantitative evaluation of glycogen concentration in bioethanol feedstock Synechocystis sp.PCC6803 using a near-infrared hyperspectral imaging system with a new near-infrared spectral camera. *Appl. Spectrosc.* **71**, 1–9.

Kacmar, J., Carlson, R. & Balogh, S. J. 2005 Staining and quantification of poly-3-hydroxybutyrate in Saccharomyces cerevisiae and Cupriavidus necator cell populations using automated flow cytometry. *Cytometry A* **69A**, 27–35.

Karan, H., Funk, C., Grabert, M., Oey, M. & Hankamer, B. 2019 Green bioplastics as part of a circular bioeconomy. *Trends Plant Sci.* **24**, 237–249.

Karmann, S., Follonier, S., Bassas-Galia, M., Panke, S. & Zinn, M. 2016 Robust at-line quantification of poly(3-hydroxyalkanoate) biosynthesis by flow cytometry using a BODIPY 493/503-SYTO 62 double-staining. *J. Microbiol. Methods* **131**, 166–171.

Khan, S. A., Sharma, G. K., Malla, F. A., Kumar, A. & Rashmi Gupta, N. 2019 Microalgae based biofertilizers: a biorefinery approach to phycoremediate wastewater and harvest biodiesel and manure. *J. Cleaner Prod.* **211**, 1412–1419.

Koch, M., Doello, S., Gutekunst, K. & Forchhammer, K. 2019 PHB is produced from glycogen turn-over during nitrogen starvation in Synechocystis sp. PCC 6803. *Int. J. Mol. Sci.* **20** (8). doi:10.3390/ijms20081942.

Lanham, A. B., Ricardo, A. R., Coma, M., Fradinho, J., Carvalheira, M., Oehmen, A., Carvalho, G. & Reis, M. A. M. 2012 Optimisation of glycogen quantification in mixed microbial cultures. *Bioresour. Technol.* **118**, 518–525.

Lanham, A. B., Rita, A., Albuquerque, M. G. E., Pardelha, F., Carvalheira, M., Coma, M., Fradinho, J., Carvalho, G., Oehmen, A. & Reis, M. A. M. 2013 Determination of the extraction kinetics for the quantification of polyhydroxyalkanoate monomers in mixed microbial systems. *Process Biochem.* **48**, 1626–1634.

Li, Q., He, X., Wang, Y., Liu, H., Xu, D. & Guo, F. 2013 Review of spectral imaging technology in biomedical engineering: achievements and challenges. *J. Biomed. Opt.* **18** (10), 100901. doi:10.1117/1.JBO.18.10.100901.

Lian, L., Hu, X., Huang, Z., Hu, L. & Xu, L. 2021 Pigment analysis based on a line-scanning fluorescence hyperspectral imaging microscope combined with multivariate curve resolution. *PLoS ONE* **16** (8), e0254864.

Markou, G., Angelidaki, I. & Georgakakis, D. 2012 Microalgal carbohydrates: an overview of the factors influencing carbohydrates production, and of main bioconversion technologies for production of biofuels. *Appl. Microbiol. Biotechnol.* **96**, 631–645.

Montiel-Jarillo, G., Carrera, J. & Suárez-Ojeda, M. E. 2017 Enrichment of a mixed microbial culture for polyhydroxyalkanoates production: effect of pH and N and P concentrations. *Sci. Total Environ.* **583**, 300–307.

O'Shea, R. E. Pahlevan, N., Smith, B., Bresciani, M., Egerton, T., Giardino, C., Li, L., Moore, T., Ruiz-Verdu, A., Ruberg, S., Simis, S. G. H., Stumpf, R. & Vaičiūtė, D. 2021 Advancing cyanobacteria biomass estimation from hyperspectral observations: Demonstrations with HICO and PRISMA imagery. *Remote Sensing of Environment* **266**, 112693. ISSN 0034-4257.

Porras, M. A., Cubitto, M. A. & Villar, M. A. 2016 Anew way of quantifying the production of poly(hydroxyalkanoate)s using FTIR. *J. Chem. Technol. Biotechnol.* **91**, 1240–1249.

Renuka, N., Guldhe, A., Prasanna, R., Singh, P. & Bux, F. 2018 Microalgae as multi-functional options in modern agriculture: current trends, prospects and challenges. *Biotechnol. Adv.* **36**, 1255–1273. http://dx.doi.org/10.1016/j.biotechadv.2018.04.004.

Rueda, E., García-Galán, M. J., Díez-Montero, R., Vila, J., Grifoll, M. & García, J. 2020a Polyhydroxybutyrate and glycogen production in photobioreactors inoculated with wastewater borne cyanobacteria monocultures. *Bioresour. Technol.* **295**, 122233.

Rueda, E., García-Galán, M. J., Ortiz, A., Uggetti, E., Carretero, J., García, J. & Díez-Montero, R. 2020b Bioremediation of agricultural runoff and biopolymers production from cyanobacteria cultured in demonstrative full-scale photobioreactors. *Process Saf. Environ. Prot.* **139**, 241–250.

Samek, O., Obruča, S., Šiler, M., Sedláček, P., Benešová, P., Kučera, D., Márova, I., Ježek, J., Bernatová, S. & Zemánek, P. 2016 Quantitative Raman spectroscopy analysis of polyhydroxyalkanoates produced by Cupriavidus necator H16. *Sensors* **16**, 1808.

Singh, A. K., Sharma, L., Mallick, N. & Mala, J. 2017 Progress and challenges in producing polyhydroxyalkanoate biopolymers from cyanobacteria. *J. Appl. Phycol.* **29**, 1213–1232.

Slonecker, T., Bufford, B., Graham, J., Carpenter, K., Opstal, D., Simon, N. & Hall, N. 2021 Hyperspectral reflectance characteristics of cyanobacteria. *Adv. Remote Sens.* **10**, 66–77.

Sonani, R. R., Rastogi, R. P. & Madamwar, D. 2017 Natural antioxidants from algae: a therapeutic perspective. In: *Algal Green Chemistry. Recent Progress in Biotechnology*. pp. 91–120.

Troschl, C., Meixner, K. & Drosg, B. 2017 Cyanobacterial PHA production – review of recent advances and a summary of three years' working experience running a pilot plant. *Bioengineering (Basel)* **4** (2), 26. doi:10.3390/bioengineering4020026.

Vermaas, W., Timlin, J., Jones, H., Sinclair, M., Nieman, L., Hamad, S., Melgaard, D. & Haaland, D. 2008 In vivo hyperspectral confocal fluorescence imaging to determine pigment localization and distribution in cyanobacterial cells. *PNAS* **105** (10), 4050-5.

Wojtasiewicz, B. & Stoń-Egiert, J. 2016 Bio-optical characterization of selected cyanobacteria strains present in marine and freshwater ecosystems. *J. Appl. Phys.* **29**, 2299–2314.

First received 7 May 2022; accepted in revised form 14 June 2022. Available online 21 June 2022